Geometric characteristics of slope toppling failure and its interpretation

Jiayuan Cao[1,2,3], Fengshan Ma[1,2,*], Jiamo Xu[1,2], Jie Guo[1,2] and Rong Lu[1,2,3]

[1]Key Laboratory of Shale Gas and Geoengineering, Institute of Geology and Geophysics, Chinese Academy of Sciences, Beijing 100029, China
[2]Institutions of Earth Science, Chinese Academy of Sciences, Beijing 100029, China
[3]University of Chinese Academy of Sciences, Beijing 100049, China

Several studies have simulated and studied the phenomenon of toppling failure caused by open-pit excavation. However, these studies do not involve or neglect the interpretation of some special geometric characteristics and laws of this deformation. Only by understanding the subtle geometric characteristics and geometric laws of slope toppling failure, can we understand the conditions, processes and mechanisms of such deformation. In this study, a soft material, small model, deformable element method is successfully used to simulate the phenomenon of the bending each layer element from the lower part of the slope to the upper, with the dislocation distance (scraps on the slope) being bigger. This method overcomes the shortcoming of the rigid body element that traditional methods cannot simulate. Finally, the conditions and mechanism of this phenomenon are further analysed and explained by structural unit of inclined composite cantilever and elastic theory. Under the action of the body force component f_x which is parallel to the longitudinal direction of the cantilever, the geometric characteristics of the single cantilever in the composite cantilever are changed such that the upper part of it is narrowed and the lower part of it is widened. Under the action of the body force component f_y which is perpendicular to the longitudinal direction of the cantilever, the cantilever is bent. Under the action of these two body force components, the composite cantilever is bent as a whole after open-pit excavation. Because of the change in the geometric shape of the cantilever, any single cantilever has a larger deflection than the other single cantilever below it; that is, greater the deflection of each cantilever along the slope upwards, greater is the curvature of the corresponding point. Finally from the lower part of the slope to the upper, the scraps on the slope are bigger.

Keywords: Cantilever beam, elastic theory, geometric characteristics, rigid body element, soft material small model, toppling failure.

WITH the increasing strength and scale of mine and hydropower construction, the problem of the toppling failure has increased for engineers and technicians. In China, examples of the typical toppling failure are Fushun West open pit mine, Yunnan Xiaolong Tan cloth dam open pit mine, Jinchuan open pit mine and Longtan Hydropower Station and so on[1–3]. This failure can be classified into two principal types, namely, flexural-toppling and block-toppling[4]. In this paper, we are mainly talking about the former. If a rock mass is composed of a set of parallel discontinuities that dip steeply against the face slope, i.e. an anti-inclined rock slope, the rock mass will act in the same manner as a set of rock columns that are placed on top of each other. If the maximum tensile stress in each rock column exceeds its tensile strength, then the rock slope will fail and topple. Such instability is categorized as flexural-toppling failure[5–8]. Physical modelling and numerical modelling are two common approaches to practically studying toppling failure of jointed rock slopes. For example, Adhikary *et al.*[9] and Zhang *et al.*[10] used centrifuge tests to explore the underlying mechanism of flexural toppling. Through physical modelling experiments, Huang *et al.*[11] revealed the correlation between deformation depth and slope angle and strata dip. Discontinuum-based methods such as distinct element code (UDEC) have achieved great success in accounting for the kinematics of discrete blocks and have been widely used to investigate the toppling failure mechanisms of rock slope. Pritchard[12] used UDEC to model the failure mechanism of flexural toppling. Cheng[13] analysed the influence of slope structure, mechanical parameters of rock mass and strata as well as initial stress on bending and toppling deformation using 3DEC. These solutions represent useful advances in the techniques for evaluating flexural-toppling mechanisms. Meanwhile, it has some shortcomings as well, e.g. centrifuge tests are as economically costly and time-consuming as other physical tests. Furthermore, when setting up the corresponding numerical model, many assumptions must be made, and inconsistencies might occur during this procedure.

In practice, all open pit mines have common geometric characteristics after excavation; that is, from the lower part of the slope to the upper, the dislocation distance between the layer elements separated by the weak structure surface (scraps on the slope) is bigger. This kind of micro geomorphology has rarely been noticed, and many scholars regard the toppling element as a rigid element to study the law of toppling failure[4]. This results in a different phenomenon from the deformable body element,

*For correspondence. (e-mail: fsma@mail.iggcas.ac.cn)

that is, from the lower part of the slope to the upper, scraps on the slope are smaller. In addition, because the elastic modulus of the selected materials of numerical and physical simulation methods is large, the micro geomorphology cannot be observed directly with the naked eye. Only by understanding the subtle geometric characteristics and geometric laws of slope toppling failure, can we understand the conditions, processes and mechanisms of such deformation. So in this article, a soft material, small model, deformable element method is successfully used to simulate the phenomenon that from the lower part of the slope to the upper, scraps on the slope are bigger. The conditions and mechanism of this phenomenon are further analysed and explained by the structural unit of inclined composite cantilever beam and elastic theory.

Physical simulation of slope toppling failure induced by open-pit excavation

Selection and manufacture of model materials

To overcome some shortcomings of existing model materials, this physical model experiment adopted a kind of soft material which is composed of gelatin, glycerin, and water of appropriate quantities. The elastic modulus of the material can be changed by adjusting the ratio of the material. In this experiment, the elastic modulus, Poisson ratio and density were about 0.02 MPa, 0.43 and 1140 kg/m^3 respectively. Hence, the material has very low elastic modulus and large Poisson's ratio. According to the similarity principle, the deformation amplitude of the slope is inversely proportional to its elastic modulus. The elastic modulus of the material is so small that the geometrical characteristics of the macroscopic deformation of slope can be shown by the small model at its body force condition of self-weight. In addition, this soft material also has the advantages of light weight and short experimental time. Usually, it takes only 1–2 days to carry out an experiment.

Experimental design

In order to study the toppling failure caused by open-pit excavation, the experiment is shown in Figure 1 below. The mould dimension is $45 \times 30 \times 0.3$ cm, and limited between two parallel tempered glass windows. The distance between the tempered glass windows is equal to the thickness of the mould, so that the model satisfies the condition of plane strain. During the experiment, as much glycerin was added as possible between the tempered glass windows and the mould so as to eliminate the friction between them. There are a total of 28 anti-dip structural planes in the model slope. The length of the structure is 6 cm, and the dip angle is 60 degrees. The distance between adjacent structures is 1 cm. The slope angle is 45 degrees.

Observations and analysis of experimental phenomena

Setting up the model after open-pit excavation, the transparent retracting figure of the model is shown in Figure 2. It can be seen that after open-pit excavation, the slope rock mass toppled due to its body force condition of self-weight. All unit bodies moved in a normal faulting manner. Wedge fissure appeared on the top platform of the slope (this is because the horizontal dimension of the model is not big enough). Crack propagation occurred at the tip of some discontinuous surfaces. Due to the full application of lubricants between all discontinuous surfaces, the frictional resistance between the surfaces is greatly reduced, so that the shear strength of every point on the surface is close to zero. That is to say, in this case, the discontinuous surface can only transmit the vertical force perpendicular to it, but not the shear surface force. At this point, the orientation of the maximum and

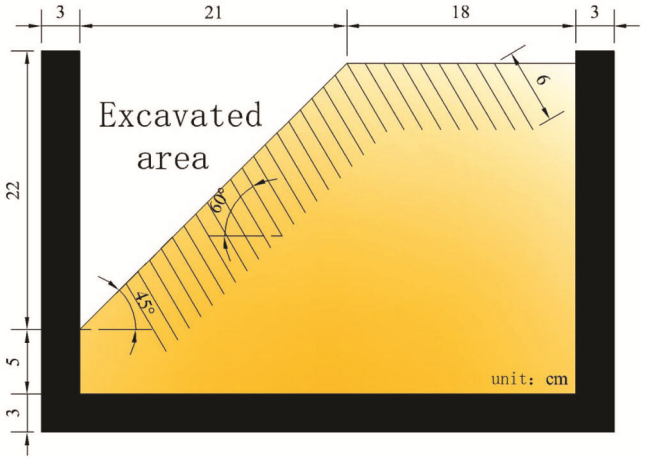

Figure 1. Schematic illustration showing the design of physical experiment for toppling deformation.

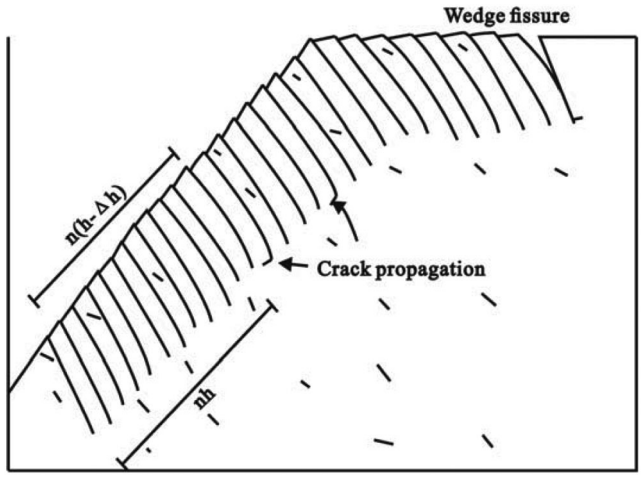

Figure 2. Transparent retracting figure of the model.

minimum two principal stresses at any point near the two sides of the discontinuous surface are perpendicular to the cross section or parallel to the cross section, but not in oblique intersection. In the area outside the discontinuous surface, the closer to the point of discontinuous surface, the more obvious is this feature of geometric characteristic. As the point moves away from the discontinuous surface, or as the distance between the two increases, this characteristic, to a significant degree, also decreases.

Explanation of phenomenon

The local isochromatic distribution of the model slope body in photoelastic apparatus is shown in Figure 3. From the different levels of isochromatic distribution in Figure 3, it is obvious that the stress distribution of the stress field in the model slope has a remarkable characteristic of principal compressive stress which is perpendicular to the layer element interface and becomes small along the downward direction of the slope. This means that the distribution of the main compressive stress on the interface between the adjacent layer elements along the downward direction of the slope has the same characteristic. An interesting phenomenon is that from the lower to upper part of the slope, dislocation distance (scraps on the slope) is bigger. This is completely different from the geometric features presented in the toppling model by Goodman[4]. Why are the results of the two experiments completely different? Through further analysis and research, the key to solving this problem is to determine whether the layer elements involved in partial toppling deformation of slope body deform. We must note that Goodman[4] used rigid elements that cannot be deformed. Therefore, no matter how small the elastic modulus of the rock body is and how much the degree of bending of layer elements is, the dislocation distance (scraps on the slope) does not become big along the upward direction of the slope. However, the rock masses in nature are all deformable bodies; so it is unreasonable to consider the rock mass as a rigid body to analyse engineering geology problems.

What caused the interesting phenomenon of the dislocation distance (scraps on the slope) to be bigger from the lower part of the slope to the upper. The explanation is as follows.

In this study, layer elements with a certain thickness separated by a set of weak structure surface are compared to special layer elements with cantilever properties. Obviously, this is a question of plane bending, which can be studied by section. The entire surface of the slope can be regarded as a combined cantilever system under the action of gravity. The deformation of each cantilever is both independent and restricted by the other cantilever. The structural element of the cantilever is used to analyse the deformation mechanism. External forces on each cantilever are shown in Figure 4. It can be decomposed into three parts: *a*, *b* and *c*. According to the superposition principle, the total external force causes the deformation effect of the cantilever, which is equal to the effect of the sum of the external forces component. The effects of external forces component are analysed below.

In Figure 4 *a*, the body force *f* of each point in the cantilever can be decomposed into body force component f_x which is parallel to the direction of the cantilever length and body force component f_y which is perpendicular to the direction of the cantilever length, as shown in Figure 5.

In order to facilitate the analysis of the deformation of the beam under the effect of body force component f_x (Figure 5 *a*2), it is assumed that the 'fixed end' of the bottom of the cantilever is disconnected and has smooth contact. Under this assumption, the displacement of every point in the cantilever can be obtained by elastic theory. The derivation is as follows.

The stress components in the cantilever are

$$\sigma_x = C_1 x + C_2;\ \sigma_y = 0;\ \tau_{xy} = 0, \tag{1}$$

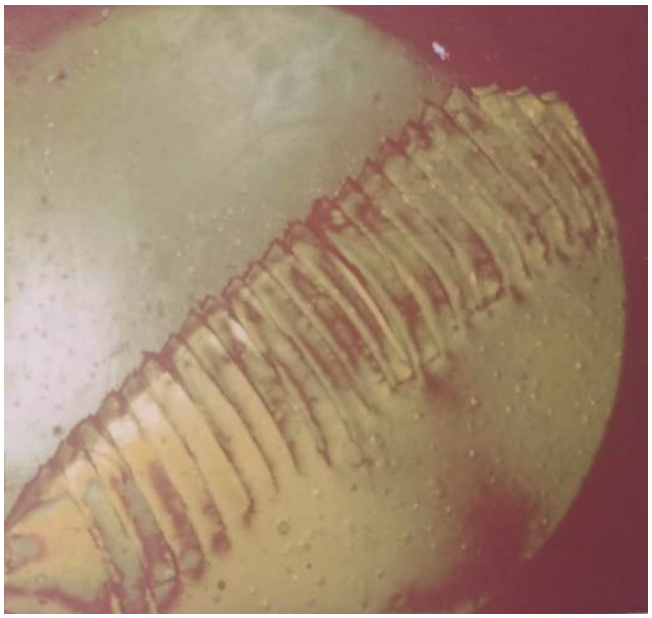

Figure 3. The local isochromatic distribution of the model slope body inphotoelastic apparatus.

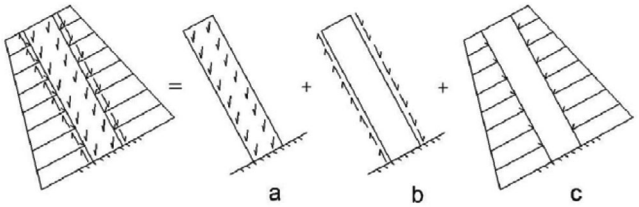

Figure 4. The decomposition of the external force of a single cantilever in the model.

when $x = 0$, $\sigma_x = -f_x l$. And when $x = l$, $\sigma_x = 0$. L is the length of the cantilever (similarly hereinafter).

Therefore, formula 1 can be rewritten as

$$\sigma_x = f_x x + -f_x l;\ \sigma_y = 0;\ \tau_{xy} = 0. \tag{2}$$

According to the physical equation represented by displacement and taking into account the plane strain condition, the following relations are

$$\begin{cases} \dfrac{\partial u}{\partial x} = \dfrac{(1-\mu^2) f_x}{E}(x-l) \\ \dfrac{\partial v}{\partial y} = \dfrac{-(1+\mu)\mu f_x}{E}(x-l) \end{cases}. \tag{3}$$

Integrate x and y from both sides of the above two equations respectively, and according to the boundary conditions, when $x = 0$, $u = 0$, $f_1(y) = 0$. When $y = 0$, $v = 0$, $f_2(x) = 0$. Therefore, the displacement expression is:

$$\begin{cases} u = \dfrac{(1-\mu^2) f_x}{E}\left(\dfrac{x^2}{2} - lx\right) \\ v = \dfrac{-(1+\mu)\mu f_x}{E}(xy - ly) \end{cases}. \tag{4}$$

According to eq. (4), the outer contour of the cantilever after deformation can be obtained as shown in Figure 6. It can be seen that under the effect of body force component f_x, the shape of the cantilever has a geometric feature such that the upper part of it is narrowed and the lower part of it is widened.

In the case of *a*2 in Figure 5, as shown in Figure 7, the surface force of any surface element (volume element with thickness of 1) in the cantilever is $-f_y \mathrm{d}x\mathrm{d}y$ (the dimension of f_y is determined by the dimension of the element). For convenience of calculation, the coordinate $y'o't$ is attached, as shown in Figure 7 *b*. Therefore, the bending moment $m(x)$ of surface element force $-f_y \mathrm{d}x\mathrm{d}y$ to any point x is equal to bending moment $m(o')$ of surface element force $-f_y \mathrm{d}x\mathrm{d}y$ to point o', that is

$$m(x) = m(o') = -f_y \cos\alpha \mathrm{d}t\mathrm{d}y\sqrt{t^2 - y^2}.$$

where α is the angle between $o't$ and the connection between o' and the centre of the surface element. The bending moment of body force component f_y for a certain point is

$$M(x) = \int_{-h/2}^{h/2}\int_{0}^{l-x} -f\cos\alpha\sqrt{t^2 + g^2}\,\mathrm{d}t\mathrm{d}y.$$

Because of $\cos\alpha = t/\sqrt{t^2 + y^2}$ the upper formula can be changed to

$$M(x) = \int_{h/2}^{h/2}\int_{2}^{l-x} -f_y t\mathrm{d}t\mathrm{d}y = -\frac{h(l-x)^2}{2} f_y.$$

The maximum bending moment $M_{\max}(o) = (hl^2/2) f_y$, angle of rotation of each point $\theta = (1/EJ)[M(x)\mathrm{d}x + C]$.

Therefore, the single cantilever bent under the action of body force component f_y.

Through the mechanical analysis of the single cantilever, it is found that under the action of body force f, it bends and its morphology changes. The final shape of the cantilever is shown in Figure 8. If the width of each cantilever

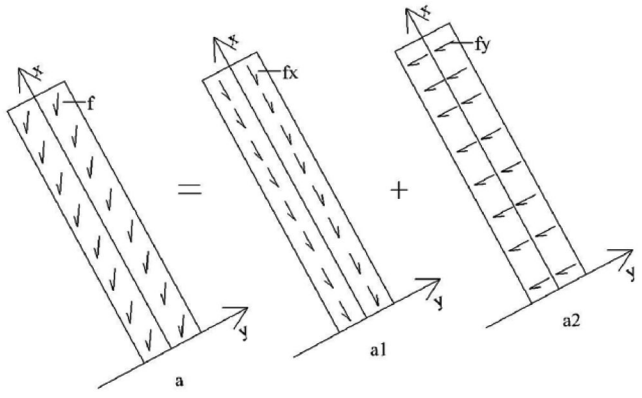

Figure 5. Decomposition of body force in a cantilever.

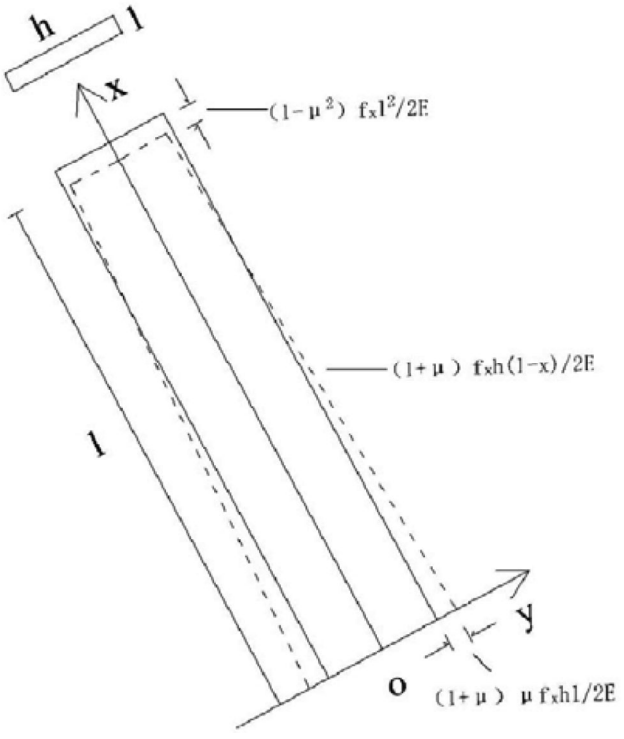

Figure 6. Deformation of cantilever under body force component f_x. which is parallel to the longitudinal direction of the cantilever.

(dimension perpendicular to the long axis of the cantilever) is unchanged before and after bending, the dislocation distance (scraps on the slope) is still equal regardless of the degree of bending of the composite cantilevers. It is like applying moment to the binding axis of a book where all pages have the same deflection. That is to say, if the thickness of all pages is the same, after bending, the ends of any two adjacent pages will have the same dislocation distance. For deformable bodies, deformation due to the body force shows that the shape of a single cantilever is not of equal thickness. In other words, the width of each cantilever changed with different amplitude, with a geometric feature since that the upper part of it is narrowed and the lower part of it is widened. At the same time, after bending, the right edge of the single cantilever bent convex outward, and the left edge of it bent convex inward. Under these conditions, if the composite cantilever was bent and any adjacent two beams maintained a fitting relationship, such a single cantilever has a larger deflection than the other single cantilevers below. That is, the deflection of the cantilever became large along the upward direction of the slope; so is the curvature. Under such conditions, for the combined cantilever system with fixed ends, its dislocation distance is bigger from the lower part of the slope to the upper part. So the scraps on the slope are also bigger from the lower part of the slope to the upper part.

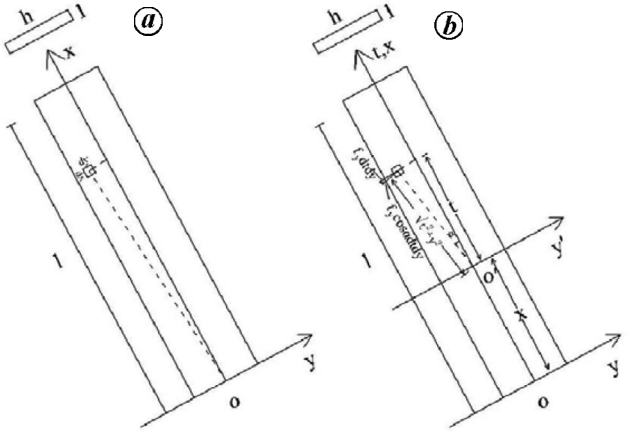

Figure 7. The mechanical analysis of Figure 6 (a2).

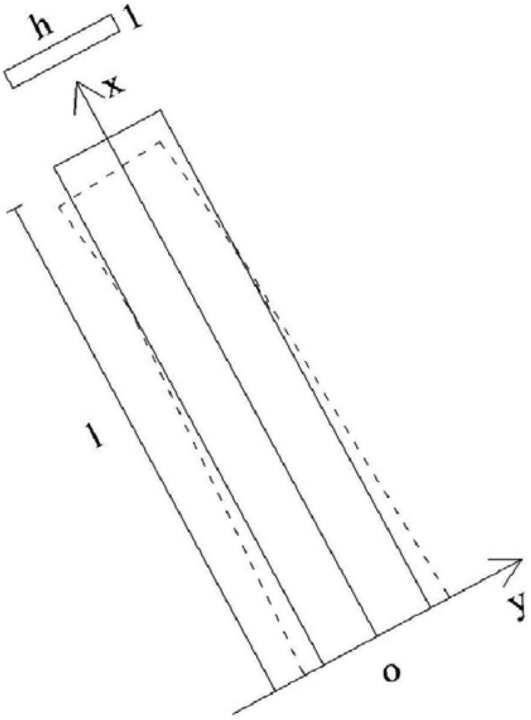

Figure 8. The final shape of the cantilever.

We can also directly measure the relative narrowing of the lower half slope from Figure 2

$$nh - n(h - \Delta h) = 22\text{ mm} - 18\text{ mm}$$

$$n\Delta h = 4\text{ mm}\ (n = 10)$$

$$\Delta h = 0.4\text{ mm}.$$

The average maximum narrowing rate for each single layer thickness is

$$\frac{\Delta h}{h} = \frac{0.4}{2.2} = 18\%.$$

These data strongly indicate that the height of each single cantilever changed greatly from the fixed end, and of course the change is gradually smaller.

It can be seen from the naked eye that the original slope in Figure 2 is much shorter, and the top platform of the original slope is much wider (that is, the position and shape of the whole slope changed in the direction of open-pit excavation), the top platform of the slope changed from the level to incline (incline to open-pit excavation) and wedge fissure occurred at the top of the slope. All these phenomena are intrinsically related to the cumulative compression deformation of the height of each cantilever along its length.

A rigid body element does not deform in the process of toppling deformation. So dislocation distance (scraps on the slope) does not become big along the upward direction of the slope.

Conclusion

In this study, a soft material, small model, deformable element method was successfully used to study the toppling failure after open-pit mining. The material used in the experiment, as a deformable body element to simulate the toppling failure caused by open-pit excavation is

closer to the actual situation of slope deformation than that of the rigid body element. So it can simulate the phenomenon of bending of each layer element and its dislocation distance (scraps on the slope) is bigger from the lower part of the slope to the upper. Based on these studies, we arrive at the following understanding.

(1) The slope rock mass with anti-dip and steep dip faults has obvious toppling deformation after open-pit excavation at its body force condition of self-weight. All the layer elements move in a normal fault way. (2) An interesting phenomenon from the lower part of the slope to the upper is that its dislocation distance (scraps on the slope) is bigger. This is completely different from the geometric features presented in the toppling model given by Goodman[4]. (3) We used structural unit of inclined composite cantilever and elastic theory to further analyse and explain the condition and mechanism of this special experimental phenomenon. The cause of this special experimental phenomenon is that layer elements separated by the weak structure surface were bent and had a geometric feature such that the upper part of it was narrowed and the lower part of it was widened after open-pit excavation. If any two adjacent beams maintained a fitting relationship, any single cantilever had a larger deflection compared to the other single cantilevers below. Finally, the dislocation distance (scraps on the slope) is bigger from the lower part of the slope to the upper part.

1. Sun, Y., *Chinese Open Pit Mine Slope Stability Analysis*, Beijing, China Science and Technology Press, 1999 (in Chinese).
2. Lu, S., The red flag range open pit mine slope toppling-displaced characteristic. In *The Chinese Typical Landslides*, Beijing, Science Press, 1988 (in Chinese).
3. Li, G., Deformation features and controlling of destabilization of western wall side-slope in Buzhaoba opencast. *Opencast Coal Min. Technol.*, 2000, (2), 11–13 (in Chinese).
4. Goodman, R. and Bray, J. W., Toppling of rock slopes. In Proceedings of the ASCE Specialty Conference on Rock Engineering for Foundations and Slopes. Boulder, CO, August 1977, pp. 201–234.
5. Amini, M., Majdi, A. and Veshadi, M. A., Stability analysis of rock slopes against block-flexure toppling failure. *Rock Mech. Rock. Eng.*, 2012, **45**, 519–532.
6. Nonomura, A. and Hasegawa, S., Regional extraction of flexural-toppled slopes in epicentral regions of subduction earthquakes along the Nankai Trough using DEM. *Environ. Earth Sci.*, 2013, **68**, 139–149.
7. Mehdi Amini, Abbas Majdi and Mohammad Amin Veshadi, Stability analysis of rock slopes against block-flexure toppling failure. *Rock Mech. Rock Eng.*, 2012, **45**, 519–532.
8. Pinheiro, A. L., Lana, M. S. and Sobreira, F. G., Use of the distinct element method to study flexural toppling at the Pico Mine, Brazil. *Bull. EngGeol. Environ.*, 2015, **74**, 1177–1186.
9. Adhikary, D. P., Dyskin, A. V., Jewell, R. J. and Stewart, D. P., A study of the mechanism of flexural toppling failure of rock slopes. *Rock Mech. Rock Eng.*, 1997, **30**(2), 75–93.
10. Zhang, J., Chen, Z. and Wang, X., Centrifuge modeling of rock-slopes susceptible to block toppling. *Rock Mech. Rock Eng.*, 2007, **40**(4), 363–382.
11. Huang, R., Wang, Z. and Xu, Q., *A Research of the Deformation and the Failure of Anti-dip Rock Slope*, Southwest Jiaotong University Press, Chengdu, 1994, pp. 62–73.
12. Pritchard, M. A. and Savigny, K. W., Numerical modeling of toppling. *Can. Geotech J.*, 1990, **27**, 824–834.
13. Cheng, D. X., Liu, D. A. and Ding, E. B., Analysis on influential factors and toppling conditions of toppling rockslope. *Chinese J. GeotechEng.*, 2005, **27**(11), 127–131.

ACKNOWLEDGEMENTS. The research supported by the Second Tibetan Plateau Scientific Expedition and Research Program (STEP) (Grant No. 2019QZKK0904), the National Key Research and Development Program of China (Grant No. 2018YFC1505301), the International Cooperation Program of Chinese Academy of Sciences (Grant No. 131551KYSB20180042).

Received 29 October 2018; revised accepted 20 December 2019

doi: 10.18520/cs/v118/i10/1569-1574